Journal of the Balkan Tribological Association *Vol. 28, No 3, 362–379* (*2022*)

ABRASIVE WEAR OF POLYMER COMPOSITE MATERIALS OBTAINED BY 3D PRINT TECHNOLOGY

PART I. POLYMER MATERIALS

M. KANDEVA[a*], N. STOIMENOV[b], M. PANEVA[b]

[a]*Faculty of Industrial Engineering, Tribology Center, Technical University – Sofia, 8 Kl. Ohridski Blvd, 1756 Sofia, Bulgaria,*
[*] *E-mail: kandevam@gmail.com*

[b]*Institute of Information and Communication Technologies – Bulgarian Academy of Sciences, Acad. G. Bonchev str., bl. 2, 1113 – Sofia, Bulgaria,*
[*] *E-mail: nikistoimenow@gmail.com*

ABSTRACT

The paper examines the parameters of abrasive wear and wear resistance of three types of polymeric materials from different manufacturers – PETG, PLA and Tough PLA, obtained by 3D technology. The materials were tested in four modes of friction – without and with lubricant grease Litol 24 and at two sliding speeds. Results and dependences for mass wear, wear rate, wear intensity and wear resistance of each material in the four friction modes were obtained. The following materials have been found out to have the best anti-wear properties: at dry friction – PETG, at sliding speed v = 0.25 m/s, at sliding speed v = 0.92 m/s – PLA; at limit lubrication with Litol 24 – PETG grease at sliding speeds v = 0.25 m/s and v = 0.92 m/s.

The results are original and have not yet been published in other editions.

Keywords: polymeric materials, 3D print technology, tribology, abrasion wear, wear resistance

* For correspondence.

AIMS AND BACKGROUND

Reducing the size of different materials for grinding is an energy-intensive and time-consuming process. Most often this process takes place in mills, which are divided into three main types: autogenous, semi-autogenous and autogenous. They are widely used in the milling of various materials such as cement, clinker, pharmaceuticals, ore mining and others[1,2,3]. Research with real-sized mills, which operate in production, is expensive. The size range is important for obtaining the desired results, which can be optimized by different means[4]. With proper consideration of the factors influencing the mills, modeling of CAD details and simulation of the motion and interaction of grinding bodies and grinding media, data close to the real ones can be obtained[5]. To take into account some factors such as friction and wear resistance, tribology is widespread. Tribological processes are also observed in the grinding processes.

One of the most rational methods for increasing the service cycle of tribotechnical systems is the use of polymer and metal-polymer materials and coatings. Such materials combine the high mechanical strength inherent in metals with the good antifriction, anti-corrosion, wear-resistant and other properties of modern polymers[6÷12].

The rapid development and improvement of three-dimensional printing or 3D printing as modern technology allow the construction of high-technology materials and three-dimensional hard details. It is radically different and it has several advantages over conventional technologies. Most traditional methods for modeling, creating and manufacturing such as casting, forging, turning, milling and more. are expensive, time-consuming and also time-consuming for most consumers[13÷18]. In papers[19, 20] the authors represent research and analysis of the main materials used in 3D print technologies. According to manufacturers, distributors and market research, the main materials are PLA (polylactic acid), PETG (Polyethylene terephthalate) and ABS (Acrylonitrile butadiene styrene). Some of the other materials are: ASA, TPE, TPU, TPC, PA, PC, PP, PEI, PVA, PVC, PEEK, HIPS and others. This requires an in-depth study of the influence of technological factors on the tribological properties of these materials such as static and kinetic coefficient of friction, wear parameters and wear resistance in different operating in case of modes – dry friction, in case of lubricated friction: abrasion, erosion, high sliding speeds, vibration, etc. Work[21] represents the results of a study of the wear characteristics in tribosystems containing biodegradable polymeric materials PLA, built by FFF / FDM 3D printing. Results were obtained for the influence of the 3D printing temperature and the friction path on the linear wear, the wear intensity and the wear resistance in a reciprocating motion (reverse friction) of the tribosystems with two types of antibodies.

The present work aims to study the characteristics of abrasive wear and wear resistance of three types of polymeric materials obtained by 3D print technology in different modes of friction – without and with lubricant at two sliding speeds.

MATERIALS

Three types of composite polymeric materials PETG, PLA and Tough PLA are studied for details obtained by 3D print technology. The details are 3D printed according to the manufacturers' recommendations, the filling of the details is set to 100% at a layer height of 0.16 mm

The designation and density of the 3D printed test materials are described in Table 1.

Table 1. Sample number, designation and density of the tested materials

No sample	Designation	Type	Density $\kappa g/m^3$
1	PETG	Polyethylene terephthalate	1145,91559
2	PLA	Polylactic acid	1145,91559
3	Tough PLA	Technical Polylactic acid	763,94373

EXPERIMENTAL

The abrasive wear test is performed by sliding a cylindrical sample of the test material on a surface with fixed abrasive particles. A tribo tester with a kinematic scheme "Pin on disk" with a functional scheme, which is shown in Fig. 1. Sample

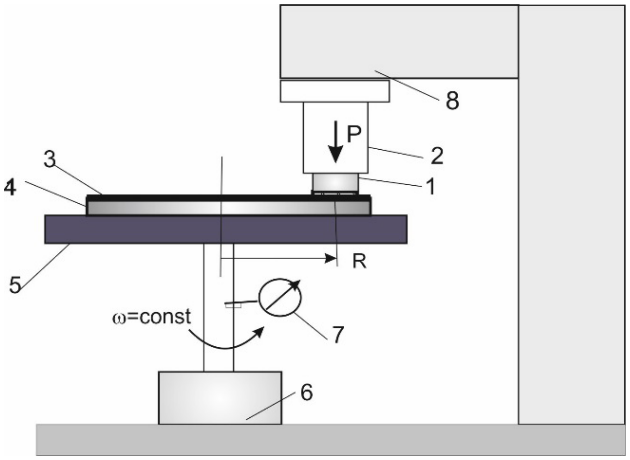

Fig. 1. Scheme of "Pin on disc" device for testing abrasive wear

1 with a diameter of 10 mm and a height of 20 mm is fixed in the holder 2 of the load head 8 so that the front surface of the sample forms a plane contact with the abrasive surface 3, which is fixed on a horizontal disk 4. The abrasive surface is modeled with impregnated Corundum P 320 with a hardness of 9,0 on the Mohs scale, which meets the requirement of the standard for at least 60% higher hardness of the abrasive surface than the hardness of the tested material. Disk 4 is driven by an electric motor 6 and it rotates around its vertical central axis at a constant angular velocity.

The normal load P in the "composite polymer-abrasive surface" tribosystem is set in the center of the contact pad between sample 1 and the abrasive surface 3 using a lever system.

The sliding path L is measured as a number of cycles (N), which are set and read with cyclometer 7. The device allows changing the sliding speed by changing the distance R and the speed of rotation of the disk.

The sliding path at the center of the contact pad for the number of cycles N is calculated by the formula:

$$L = 2\pi R.N \tag{1}$$

where R is the distance from the axis of rotation of the disk to the center of the contact pad (Fig. 1).

The parameters of the experimental study are represented in Table 2.

Table 2. Experiment parameters

No	Parameter	Value
1	Normal load	4.9 N = const
2	Nominal contact area	78.5 x 10^6 m^2
3	Nominal contact pressure	6.2 x 10^4 N/m^2 = const
4	Sliding speeds	V = 0.25 m/s; V = 0.92 m/s
5	Abrasive surface	Corundum P 320
6	Lubricant	Grease Litol 24
7	Environmental temperature	22^o C

The research methodology consists in measuring the mass wear of a sample of the test material during a certain friction path (number of cycles) under given constant conditions – sliding speed, normal load, type of abrasive surface, environmental temperature. Mass wear (m) is defined as the difference between the initial mass of the sample (before friction) and the mass of the sample after a certain friction path length and it is measured with an electronic weighing scale WPS 180/C/2 accuracy of 0.1 mg. Before each mass measurement, the sample is cleaned of mechanical and organic particles and dried with ethyl alcohol to prevent the electrostatic effect. The abrasive surface is replaced on each sample.

After measuring the mass wear (m), the wear characteristics are calculated: wear rate, wear intensity and wear resistance.

The rate of mass wear is the fractured mass of the sample surface per unit of time of friction and it is measured in mg/min:

$$\gamma = \frac{m}{t} \tag{2}$$

The relationship between the measured mass wear *m* and the linear wear *h* of the sample (normal wear to the sliding velocity vector) is represented by the formula:

$$h = \frac{m}{\rho . A_a} \tag{3}$$

where $A_a = \pi r^2$ is the nominal friction contact area, where *r* is the radius of the contact pad; ρ – coating density.

The intensity of abrasive wear i_a represents linear wear *h* of the sample per unit of friction path length, ie.

$$i_a = \frac{m}{\rho . A_a . L} \tag{4}$$

Absolute wear resistance I_r is represented as a reciprocal of the wear intensity, ie.

$$I_r = \frac{1}{i_a} = \frac{\rho . A_a . L}{m} \tag{5}$$

Wear intensity and wear resistance are dimensionless numbers.

The tested 3 types of materials are tested in four modes of friction:

- Dry friction with sliding speed of 0.25 m/s;
- Dry friction with sliding speed of 0.92 m/s;
- Friction with grease Litol 24 with sliding speed 0.25 m/s;
- Friction with grease Litol 24 with sliding speed 0.92 m/s;

RESULTS AND DISCUSSION

With the described methodology and device, results were obtained for the wear characteristics of each of the tested materials. The results are represented below in tabular and graphical form for each material separately. The wear rate, wear intensity, and wear resistance are calculated by formulas (2), (4), and (5).

Examination of PETG material – Sample No 1

Tables 3 and 4 represent the results for mass wear, wear rate, wear intensity and wear resistance of PETG material in dry friction and when lubricated with grease Litol 24 at both sliding speeds, respectively v=0.25 m/s (n=60 min^{-1}) and v=0.25 m/s (n=220 min^{-1}).

Table 3. Wear characteristics of PETG material in friction modes without and with lubricant at a sliding speed of 0.25 m/s

Sample No 1 – PETG Dry friction, V=0.25 m/s				
Number of cycles (N)	**200**	**400**	**600**	**800**
Sliding distance, m	**50**	**100**	**150**	**200**
Sliding time, min	**3.3**	**6.6**	**9.9**	**13.2**
Mass loss, mg	12.3	25.8	34.2	38.0
Wear speed, mg/min	3.7	3.9	3.5	2.9
Wear intensity	$2.7x10^{-6}$	$2.9x10^{-6}$	$2.5x10^{-6}$	$2.1x10^{-6}$
Wear resistance	$0.37x10^{6}$	$0.35x10^{6}$	$0.4x10^{6}$	$0.48x10^{6}$
Sample No 1 – PETG With Litol 24, V=0.25 m/s				
Mass loss, mg	13.6	20.9	24.6	27.4
Wear speed, mg/min	4.1	3.2	2.5	2.1
Wear intensity	$3.0x10^{-6}$	$2.3x10^{-6}$	$1.8x10^{-6}$	$1.5x10^{-6}$
Wear resistance	$0.33x10^{6}$	$0.43x10^{6}$	$0.55x10^{6}$	$0.66x10^{6}$

Table 4. Wear characteristics of PETG material in friction modes without and with lubricant at sliding speed 0,92 m/s

Sample No 1 – PETG Dry friction, V=0.92 m				
Number of cycles (N)	**200**	**400**	**600**	**800**
Sliding distance, m	**50**	**100**	**150**	**200**
Sliding time, min	**3.3**	**6.6**	**9.9**	**13.2**
Mass loss, mg	14.7	25.4	33.7	45.0
Wear speed, mg/min	16.2	14.0	12.3	12.4
Wear intensity	$3.26x10^{-6}$	$2.81x10^{-6}$	$2.49x10^{-6}$	$2.49x10^{-6}$
Wear resistance	$0.31x10^{6}$	$0.36x10^{6}$	$0.40x10^{6}$	$0.40x10^{6}$
Sample No 1 – PETG With Litol 24, V=0.92 m/s				
Mass loss, mg	11.9	13.8	19.6	20.3
Wear speed, mg/min	13.1	7.6	7.2	5.6
Wear intensity	$2.64x10^{-6}$	$1.53x10^{-6}$	$1.45x10^{-6}$	$1.12x10^{-6}$
Wear resistance	$0.38x10^{6}$	$0.65x10^{6}$	$0.69x10^{6}$	$0.89x10^{6}$

According to the data in Tables 3 and 4, graphs of the dependences of mass wear on the sliding path in the dry friction mode (Fig. 2) and with Litol 24 grease (Fig. 3) at both sliding speeds are plotted.

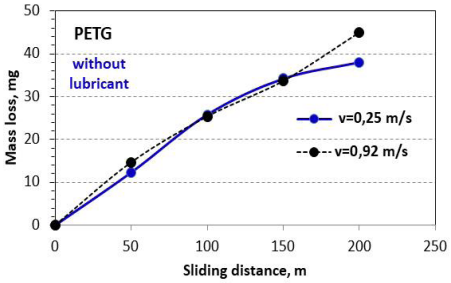

Fig. 2. Dependence of wear on the sliding path length in friction without lubrication for two speeds

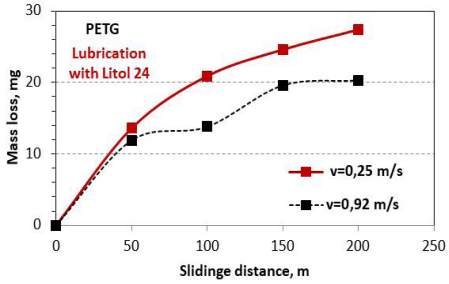

Fig. 3. Dependence of wear on the sliding path length in friction with grease Litol 24 for two speeds

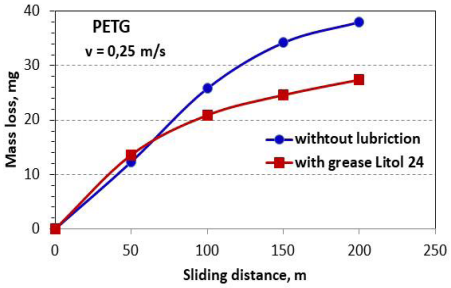

Fig. 4. Dependence of wear on the sliding path length without and with lubricant Litol 24 at v=0.25 m/s

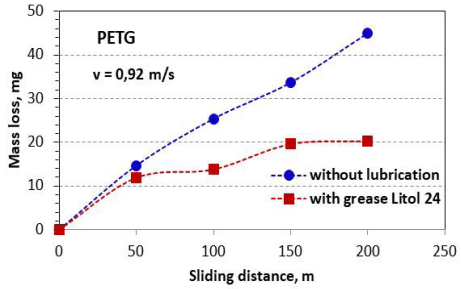

Fig. 5. Dependence of wear on the sliding path length without and with lubricant Litol 24 at v=0.92 m/s

From Fig. 2 it is seen that in dry friction for both speeds the curves overlap, ie. no difference in wear was observed in the two modes up to a friction path of 150 m, followed by wear at a higher speed of 0.92 m/s with nonlinearity in the dependences. This result is more clearly seen from the data on the change in wear intensity in Tables 3 and 4. At low speeds (0.25 m/s) the sliding intensity decreases linearly with increasing friction path length, and at high speeds after 150 m remains almost constant.

In the conditions of when lubricated (Fig. 3) the wear has smaller values and the dependences have a clearly expressed nonlinear character. It can be seen that at low sliding speeds the wear is greater than at high speeds. The intensity at low values decreases nonlinearly with the friction path length, while at high speeds after the running-in stage it remains almost constant.

In Fig. 4 and Fig. 5 it is seen wear depends on the friction path for dry and when lubricated at speeds of 0.25 m/s and 0.92 m/s, respectively. For the same friction path – 200 m at a speed of 0.25 m/s at limit lubrication wear decreases by 28%, and at 3,68 times higher sliding speed of 0.92 m/s lubrication wear is reduced by 55%.

In Fig. 6 is shown a diagram of the wear resistance of PETG material in different friction modes. It can be seen that PETG material has the highest abrasion resistance – $0.66.10^6$ in the mode (when lubricated) at low sliding speeds v = 0.25 m/s. In dry rubbing mode, the wear resistance of PETG material is twice lower – $0.35x10^6$ and it does not depend on the sliding speed.

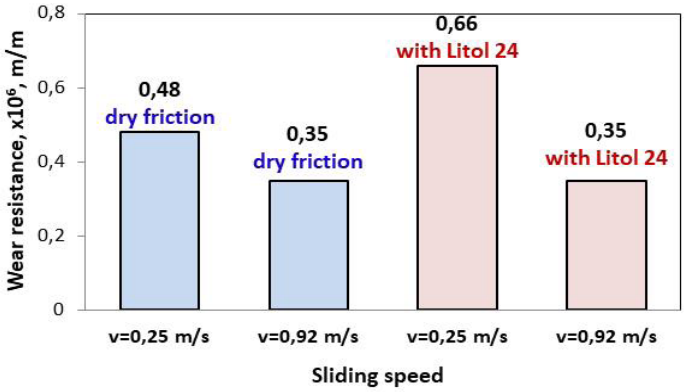

Fig. 6. Wear resistance diagram of PETG material for two sliding speeds in dry friction and lubrication with Litol 24 at friction path length 200 m

Examination of PLA material – Sample No 2

The experimental results for the wear characteristics and wear resistance of PLA material in dry and when lubricated friction regimes for both sliding speeds are represented in Tables 5 and 6.

Table 5. Wear characteristics of PLA material in friction modes without and with lubricant at a sliding speed of 0.25 m/s

Sample No 2 – PLA Dry friction, V=0.25 m/s				
Number of cycles (N)	**200**	**400**	**600**	**800**
Sliding distance, m	**50**	**100**	**150**	**200**
Sliding time, min	**3.3**	**6.6**	**9.9**	**13.2**
Mass loss, mg	14.8	30.5	44.1	52.1
Wear speed, mg/min	4.5	4.6	4.5	4.0
Wear intensity	$3.3x10^{-6}$	$3.4x10^{-6}$	$3.3x10^{-6}$	$2.9x10^{-6}$
Wear resistance	$0.30x10^6$	$0.29x10^6$	$0.31x10^6$	$0.35x10^6$

Sample No 2 – PLA With Litol 24, V=0.25 m/s				
Mass loss, mg	18.5	20.8	30.1	51.4
Wear speed, mg/min	5.6	3.2	3.0	3.9
Wear intensity	$4.1x10^{-6}$	$2.3x10^{-6}$	$2.2x10^{-6}$	$2.9x10^{-6}$
Wear resistance	$0.24x10^{6}$	$0.43x10^{6}$	$0.45x10^{6}$	$0.35x10^{6}$

Table 6. Wear characteristics of PLA material in friction modes without and with lubricant at a sliding speed of 0.92 m/s

Sample No 2 – PLA Dry friction, V=0.92 m/s				
Number of cycles (N)	**200**	**400**	**600**	**800**
Sliding distance, m	**50**	**100**	**150**	**200**
Sliding time, min	**3.3**	**6.6**	**9.9**	**13.2**
Mass loss, mg	15.1	25.6	30.5	38.4
Wear speed, mg/min	16.6	14.1	11.2	10.5
Wear intensity	$3.35x10^{-6}$	$2.84x10^{-6}$	$2.25x10^{-6}$	$2.13x10^{-6}$
Wear resistance	$0.30x10^{6}$	$0.35x10^{6}$	$0.44x10^{6}$	$0.47x10^{6}$
Sample No 2 – PLA With Litol 24, V=0.92 m/s				
Mass loss, mg	14.7	16.8	31.2	44.3
Wear speed, mg/min	16.2	9.2	11.4	12.2
Wear intensity	$3.26x10^{-6}$	$1.86x10^{-6}$	$2.3x10^{-6}$	$2.45x10^{-6}$
Wear resistance	$0.31x10^{6}$	$0.54x10^{6}$	$0.43x10^{6}$	$0.41x10^{6}$

In Fig. 7 is shown the kinetic curve of dry friction wear. It is clear that, in contrast to the PETG composite material, at high sliding speeds the wear is significantly less than at low speeds and the dependence is almost directly proportional.

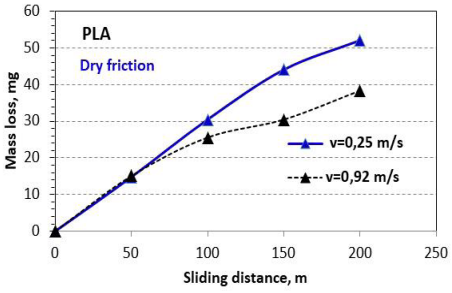

Fig. 7. Dependence of wear on the sliding path length in friction without lubrication for two speeds

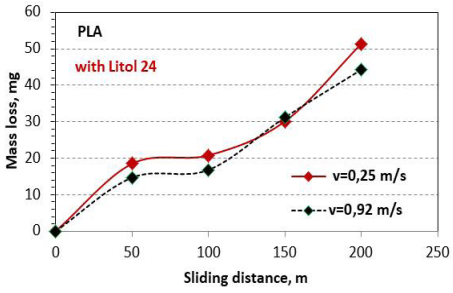

Fig. 8. Dependence of wear on the sliding path length in friction with grease Litol 24 for two speeds

The data in Tables 5 and 6 show that the wear intensity at low sliding speed is higher and gradually decreases with the friction path length. At high sliding speeds, the wear intensity decreases exponentially.

In the limit lubrication mode, the dependence of wear on the friction path length is exponential at both sliding speeds and is higher at low sliding speeds – 0.25 m/s (Fig. 8). The kinetics of the process is different for the two sliding speeds. Up to a friction path of 100 m, the wear remains constant, after which it increases at different speeds. This is more clearly understood from the values of wear intensity. At both sliding speeds up to a certain friction path length (100 m), the wear intensity decreases sharply and then begins to increase. The dependence is highly nonlinear, which indicates the instability of the friction processes in the presence of a lubricant. At this stage of the study, it can be assumed that these processes are due to tribochemical reactions in the contact, accompanied by intensive deformation and micro-cutting in the surface layer of the material. After wear on the edges of the sample, threads of the material with a length of about 2-4 mm were observed.

In Figures 9 and 10 the graphs show the change in wear from the sliding path length for dry friction and when lubricated for both speeds.

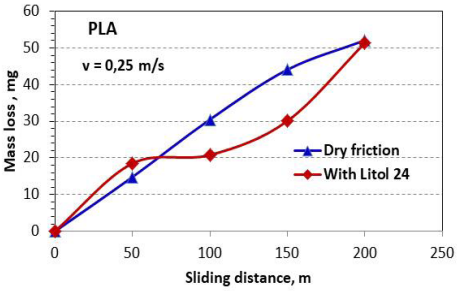

Fig. 9. Dependence of wear on the sliding path length without and with lubricant Litol 24 at v=0.25 m/s

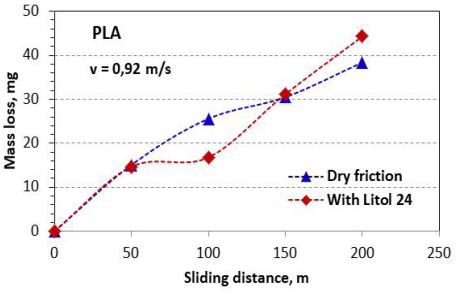

Fig. 10. Dependence of wear on the sliding path length without and with lubricant Litol 24 at v=0.92 m/s

The wear resistance diagram in Fig. 11 shows that the highest wear resistance material PLA has in the modes of dry friction – 0.47×10^6 and when lubricated – 0.41×10^6 at a high sliding speed of 0.92 m/s. At low speeds – 0.25 m/s the presence of lubricant does not affect the wear resistance, it is the same for dry and when lubricated friction – 0.35×10^6.

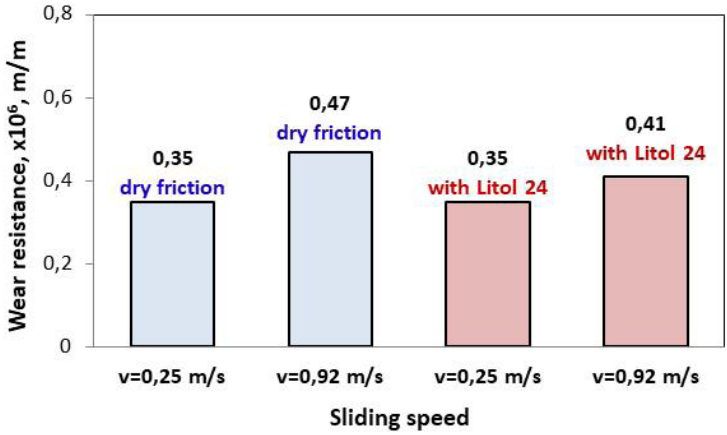

Fig. 11. Wear resistance diagram of PLA material for two sliding speeds in dry friction and lubrication with Litol 24 at friction path length 200 m

Study of material Tough PLA – Sample № 3

The experimental results for mass wear, wear rate, wear intensity and wear resistance of Tough PLA material under friction without and with lubricant for two sliding speeds are represented in Tables 7 and 8.

Table 7. Wear characteristics of Tough PLA material in friction modes without and with lubricant at a sliding speed of 0.25 m/s

Sample № 3 – Tough PLA Dry friction, V=0.25 m/s				
Number of cycles (N)	**200**	**400**	**600**	**800**
Sliding distance, m	**50**	**100**	**150**	**200**
Sliding time, min	**3.3**	**6.6**	**9.9**	**13.2**
Mass loss, mg	27.2	43.4	58.0	64.3
Wear speed, mg/min	8.2	6.6	5.9	4.9
Wear intensity	9.0×10^{-6}	7.2×10^{-6}	6.4×10^{-6}	5.3×10^{-6}
Wear resistance	0.11×10^{6}	0.14×10^{6}	0.16×10^{6}	0.19×10^{6}
Sample № 3 – Tough PLA With Litol 24, V=0.25 m/s				
Mass loss, mg	21.1	40.8	59.3	67.7
Wear speed, mg/min	6.4	6.2	6.0	5.1
Wear intensity	7.0×10^{-6}	6.8×10^{-6}	6.6×10^{-6}	5.6×10^{-6}
Wear resistance	0.14×10^{6}	0.15×10^{6}	0.15×10^{6}	0.18×10^{6}

Table 8. Wear characteristics of Tough PLA material in friction modes without and with lubricant at sliding speed 0.92 m/s

Sample № 3 – Tough PLA Dry friction, V=0.92 m/s				
Number of cycles (N)	**200**	**400**	**600**	**800**
Sliding distance, m	**50**	**100**	**150**	**200**
Sliding time, min	**3.3**	**6.6**	**9.9**	**13.2**
Mass loss, mg	19.4	24.7	32.4	38.3
Wear speed, mg/min	21.3	13.6	13.7	10.5
Wear intensity	6.44×10^{-6}	4.1×10^{-6}	3.59×10^{-6}	3.18×10^{-6}
Wear resistance	0.16×10^{6}	0.24×10^{6}	0.28×10^{6}	0.32×10^{6}
Sample № 3 – Tough PLA With Litol 24, V=0.92 m/s				
Mass loss, mg	11.8	23.2	37.5	46.1
Wear speed, mg/min	13.0	12.7	15.8	12.7
Wear intensity	3.92×10^{-6}	3.85×10^{-6}	4.15×10^{-6}	3.83×10^{-6}
Wear resistance	0.26×10^{6}	0.26×10^{6}	0.24×10^{6}	0.26×10^{6}

Dry friction and when lubricated wear curves are shown in Fig. 12 and Fig. 13.

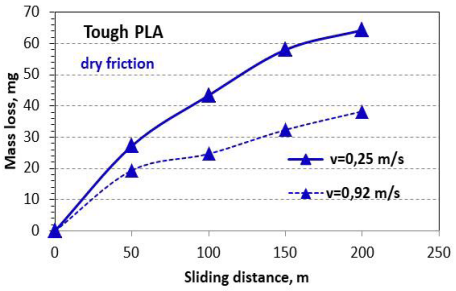

Fig. 12. Dependence of wear on the sliding path length in friction without lubrication for two speeds

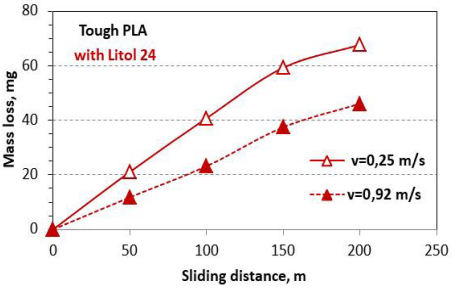

Fig. 13. Dependence of wear on the sliding path length in friction with grease Litol 24 for two speeds

In dry friction mode, the wear at higher sliding speeds is almost twice as low as the wear at low sliding speeds. The change in the wear intensity from the friction path is linear.

In "when lubricated" mode, the same trend is observed: at high sliding speeds, the wear is much less than at low speeds. This may be due to the formation of a boundary protective film on the surface of the sample as a result of the increased contact temperature at high speed and the occurrence of tribochemical reactions in the interaction of lubricant components and surface elements.

The formation of a protective film is also possible under dry friction conditions. The possibility of tribochemical reactions in combination with micro-cutting and plastic deformations depends on the nature and structure of the surface layer of the composite material, as well as on the orientation of the threads concerning the vector of the sliding speed.

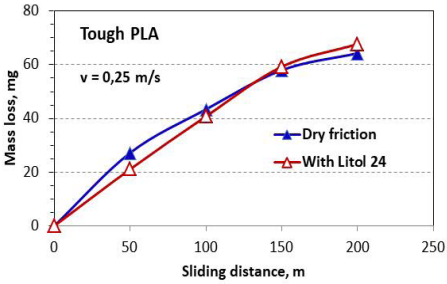

Fig. 14. Dependence of wear on the sliding path length without and with lubricant Litol 24 at v=0.25 m/s

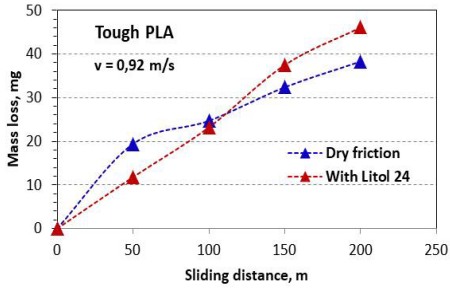

Fig. 15. Dependence of wear on the sliding path length without and with lubricant Litol 24 at v=0.92 m/s

Fig. 14 and Fig. 15 show the wear curves for dry friction and when lubricated at low speeds of 0.25 m/s and high sliding speeds of 0.92 m/s, respectively. It can be seen that the wear on the friction path at high speeds for dry and when lubricated is within the range of 38 to 45 mg, and at low speeds is over 60 mg.

The wear resistance diagram in Fig. 16 shows that the Tough PLA material has the highest abrasion resistance of 0.32×10^6 in the limit lubrication mode with Litol 24 at high sliding speeds.

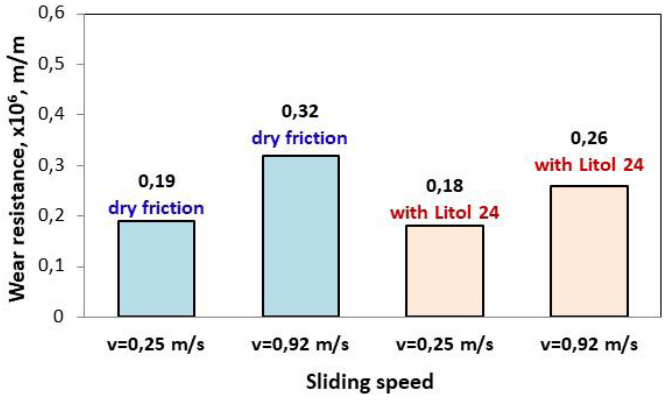

Fig. 16. Wear resistance diagram of Tough PLA material for two sliding speeds in dry friction and lubrication with Litol 24 at friction path length 200 m

Comparative results for the wear resistance of the tested materials

In Table 9 are represented data on the wear resistance of the tested polymeric materials for all modes of friction – dry and when lubricated at two sliding speeds at the same sliding path length L = 200 m.

Table 9. Wear resistance of the tested materials in dry friction and when lubricated with Litol 24 grease at two sliding speeds

Sample No	Name of the material	Wear resistance at v = 0.25 m/s; L = 200 m		Wear resistance at v = 0.92 m/s; L = 200 m	
		Dry friction	With grease Litol 24	Dry friction	With grease Litol 24
1	PETG	0.48 x 10^6	0.66 x 10^6	0.40 x 10^6	0.89 x 10^6
2	PLA	0.35 x 10^6	0.35 x 10^6	0.47 x 10^6	0.41 x 10^6
3	Tough PLA	0.19 x 10^6	0.18 x 10^6	0.32 x 10^6	0.26 x 10^6

In Fig. 17 is represented a diagram of the wear resistance of materials in dry friction modes, and Fig. 18 is represented a diagram of wear resistance when lubricated at two sliding speeds.

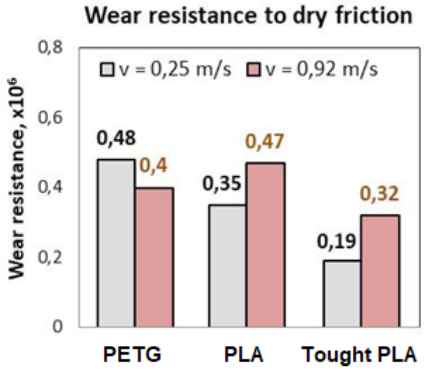

Fig. 17. Diagram of the wear resistance of the test materials in dry friction mode for two sliding speeds with a friction path length of 200 m

From the diagram in Fig. 17 it can be seen that in the dry friction mode the highest abrasion resistance has the material PETG – I_r = 0.48x10^6 at a sliding speed of 0.25 m/s. The material Tough PLA – I_r = 0.19x10^6 at the speed of 0.25 m/s and at the speed of 0.92 m/s has the lowest abrasion resistance at dry friction – I_r=0.32x10^6.

In the mode when lubricated with Litol 24, PETG material has the highest abrasion resistance at a high sliding speed of 0,92 m/s (I_r=0.89x10^6), and Tought PLA material has the lowest abrasion resistance (I_r=0.26x10^6) at the same sliding speed – Fig. 18.

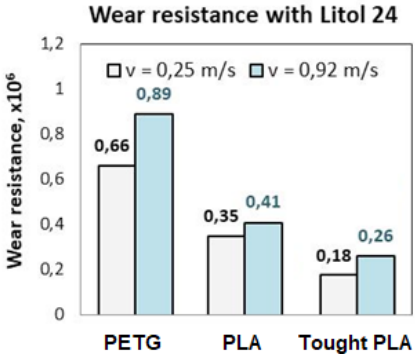

Fig. 18. Diagram of the wear resistance of the test materials when lubricated with Litol 24 for sliding speeds with a friction path length of 200 m

Figures 19 and 20 represent comparative results of the abrasion resistance of the materials under dry and when lubricated at the same sliding speed, respectively 0.25 m/s (Fig. 19) and 0.92 m/s, (Fig. 20).

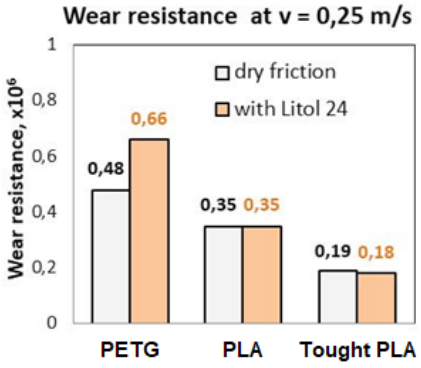

Fig. 19. Diagram of the wear resistance of the tested materials in the dry friction and lubrication with Litol 24 at a sliding speed v = 0.25 m / s and a friction path length of 200 m

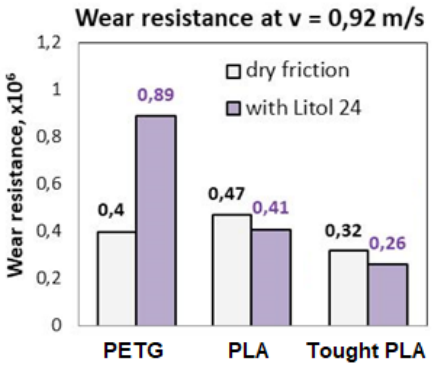

Fig. 20. Diagram of the wear resistance of the tested materials in the dry friction and lubrication with Litol 24 at a sliding speed v = 0.92 m / s and a friction path length of 200 m

From the analysis it can be concluded that of all the tested materials in the four modes of abrasive friction, the best anti-wear properties have the following materials:

- in dry friction – PETG at sliding speed v=0.25 m/s and PLA at sliding speed v=0.92 m/s;
- when lubricated with Litol 24 – PETG at sliding speed v=0.25 m/s and v=0.92 m/s.

CONCLUSIONS

In the publication are represented results on the abrasive wear characteristics of three types of composite polymeric materials – PETG, PLA and Tough PLA, the samples are obtained with the usage of 3D printing technology. The materials were tested in four modes of friction – without and with lubricant grease Litol 24 at two sliding speeds – v=0.25 m/s and v=0.92 m/s.

Results and graphical dependences for mass wear, wear rate, wear intensity and wear resistance of each material in the four modes of friction were obtained.

It was found out that the influence of the presence of lubricant and the magnitude of the sliding speed has a different nature on the obtained dependences and absolute values of the wear parameters for individual materials.

Comparative diagrams for the wear resistance of the tested materials in the four modes of friction are represented.

The following materials have been found out to have the best anti-wear properties:

– in dry friction mode – material PETG at sliding speed v=0.25 m/s and PLA at sliding speed v=0.92 m/s;

– when lubricated with Litol 24 mode – material PETG at sliding speed v=0.25 m/s and v=0.92 m/s.

ACKNOWLEDGEMENTS

This research was carried out as part of the project № KP-06-N47/5 "Research and optimization of the interaction between grinding bodies and media with an innovative shape", financed by the Bulgarian National Science Fund, and supported by the Grant No BG05M2OP001-1.002-0011 Center of Competence "MIRACle (Mechatronics, Innovation, Robotics, Automation, Clean Technologies)", financed by the Science and Education for Smart Growth Operational Program (2014-2020) and co-financed by the European Union through the European Structural and Investment funds.

REFERENCES

1. F. M. LEWIS et al.: Comminution: A Guide To Size Reduction System Design. Mining Eng, **28**, 29 (1976).
2. B. A. WILLS, J. A. FINCH: Grinding Mills: Ch. 7. Barry A. Wills, James A. Finch (Eds.). Wills' Mineral Processing Technology (Eighth Edition): Butterworth-Heinemann, 147 (2016).
3. B. A. WILLS, J. A. FINCH: Tubular Rod Mills: Ch. 8. Ashok Gupta, Denis Yan (Eds.). Mineral Processing Design and Operations (Second Edition): Elsevier, 241 (2016).
4. I. MALAKOV, V. ZAHARINOV, V. TZENOV: Size Ranges Optimization. Procedia Engineering, **100**, 791 (2015).
5. G. DINEV, I. MALAKOV, D. DOTSEV: CAD Optimal Design, Documentation and Automated Assembly of Mechanical Product. Adv Mater Res, **463-464**, 1202 (2012).
6. R. GRAS: Tribologie. Principes et Solutions Industrielles. Dunod, L'Usine Nouvelle (2008).
7. R. BASSANI: Tribology. Pisa University Press (2013).
8. N. DENISOVA, V. SHORIN, I. GONTAR, N. VOLCHIKHINA, N. SHORINA: Tribotechnical Materials Science and Tribotechnology. Penza (2006) (in Russian).
9. T. PENYASHKI, V. KAMBUROV, G. KOSTADINOV, M. KANDEVA, R. DIMITROVA, A. NIKOLOV: Some Ways to Increase the Wear Resistance of Titanium Alloys. J Balk Tribol Assoc, **27** (1), 1 (2020).
10. M. KANDEVA, Z. KALITCHIN, Y. STOYANOVA: Influence of Chromium Concentration on the Abrasive Wear of Ni-Cr-B-Si Coatings Applied by Supersonic Flame Jet (HVOF). Metals, **11**, 915 (2021). https://doi.org/10.3390/met11060915
11. M. KANDEVA, N. STOIMENOV, B. POPOV, Z. KALITCHIN, V. POZHIDAEVA: Abrasive Wear Resistance of Micro- and Nano-Diamond Particles. J Balk Tribol Assoc, **26** (2), 181 (2020).

12. V. DYAKOVA, P. TASHEV, M. KANDEVA: Study on the Effect of Nanosized Particles of Tin and SiC on the Wear Resistance, Microstructure and Corrosion Behavior of Overlay Weld Metal. J Balk Tribol Assoc, **26** (1), 56 (2020).
13. N. MYSHKIN, M. PETROKOVETS: Tribology. Principles and Applications. Gomel: IMMS NASB (2002) (in Russian).
14. D. MOORE: The Friction and Lubrication of Elastomers. Pergamon Press (1977).
15. N. K. MYSHKIN, C. K. KIM, M. I. PETROKOVETS: Introduction to Tribology. Paju: Cheong Moon Gak (1997).
16. Create it REAL Aps. https://www.createitreal.com/3d-printer-electronics/48/
17. N. STOIMENOV, D. KARASTOYANOV, L. KLOCHKOV: Study of the Factors Increasing the Quality and Productivity of Drum, Rod and Ball mills. 2nd Int. Conf. on Environment, Chemical Engineering & Materials, ECEM '18, Malta Sliema, June 22-24, 2018. AIP (American Institute of Physics) Conference Proceedings, **2022 (**1), 020024-1 (2018).
18. S. FARAH, D. G. ANDERSON, R. LANGER: Physical and Mechanical Properties of PLA, and Their Functions in Widespread Applications – a Comprehensive Review. Adv Drug Deliv Rev, **107**, 367 (2016). https://doi.org/10.1016/j.addr.2016.06.012.
19. B. POPOV, M. PANEVA, N. STOIMENOV, L. KLOCHKOV: Survey and Analysis of Materials for 3D Printing. XXX International Scientific and Technical Conference, ADP – 2021, Sozopol, Bulgaria. Automation of Discrete Production Engineering, **3**, 218 (2021).
20. 3D Jake. https://www.3djake.com/
21. M. ZAGORSKI, G. TODOROV, N. NIKOLOV, Y. SOFRONOV, M. KANDEVA: Investigation on Wear of Biopolymer Parts Produced by 3D Printing in Lubricated Sliding Conditions. Industrial Lubrication and Tribology, **74** (3), 360 (2022). DOI 10.1108/ILT-06-2021-0214

Received 20 May 2022
Revised 15 June 2022